https://doi.org/10.5564/mjc.v23i49.2049
Mongolian Journal of Chemistry
www.mongoliajol.info/index.php/MJC

Wound-healing activity of polyhexamethyleneguanidine hydrochloride hydrogel and extract of *Bergenia crassifolia* on thermal burn simulation

Sergey A. Stelmakh[1*], Oleg S. Ochirov[1], Maria N. Grigor'eva[1], Anatoly A. Tykheev[2], Svetlana N. Lebedeva[2], Valeria O. Okladnikova[1], Sesegma D. Zhamsaranova[2]

[1]*Baikal Institute of Nature Management, Siberian Branch, Russian Academy of Sciences, Sakhyanova Str., 6, Ulan-Ude 670043, Russia*
[2]*East Siberia State University of Technologies and Management 40V, Klyuchevskaya Str., 1, Ulan-Ude 670013, Russia*

** Corresponding author: s_stelmakh@bk.ru;* ORCID ID: 0000-0003-3392-5600

Received: 21 June 2022; revised: 28 November; accepted: 2 December 2022

ABSTRACT

The results of a study of the wound healing activity of a composition based on the hydrogel of polyhexamethylene guanidine hydrochloride and *Bergenia crassifolia* extract, under conditions of modeling thermal burns in laboratory animals (rats), are presented. It was found that the composition affects the change in the summary antioxidant and leukocyte activity towards the normalization of these indicators. Morphological analysis of the slices showed that, under the influence of a polyhexamethylene guanidine hydrogel composition and *B.crassifolia* extract, healing proceeds more intensively than in the control group and is manifested by a smaller thickness of the leukocyte-necrotic scab, accelerated epithelization, and complete closure of the skin defect.

Keywords: Wound healing, hydrogel, extract, polyhexamethylene guanidine hydrochloride, toxicity

INTRODUCTION

Healing of skin wounds requires the selection of an appropriate treatment based on the current stage of tissue damage. The first stage of burn wound treatment usually involves antiseptic agents that prevent the penetration of harmful microorganisms into the wound, and wound healing stimulators that exhibit anti-inflammatory properties and promote the growth of leukocytes [1]. Multicomponent industrial preparations such as ointment and gel are traditionally used for external application. These preparations are based on polyethylene oxide, polyvinyl alcohol, and polyacrylates [2, 3]. As drug carriers, polymer hydrogels have gained increasing interest [4-7]. There has been tremendous interest in polyguanidines because of their high antibacterial properties, low toxicity and ability to form highly swollen hydrogels that can be complexed [8-11]. In our previous study, we demonstrated that the gels exhibit wound-healing effects comparable to those of widely used chloramphenicol and methyluracil preparations [12, 13]. Thus, these gels can be used to design herbal or chemical medicinal products to treat skin injuries [14, 15].

With polyhexamethylene guanidine hydrochloride (PHMGH) hydrogel's high sorption activity, we anticipate the development of highly effective drugs that combine the antimicrobial and wound healing properties of both the hydrogel and plants that have been used in alternative medicine for more than a decade, including medicinal plants from the Baikal region [16].

Leaves and roots of *B.crassifolia* extract are widely used in making medicines, food and biologically active additives, balms, syrups, drinks, and herbal teas. The medicinal properties of *B.crassifolia* extract have long been used in folk medicine, as well as in Chinese and Tibetan medicine. Tuberculosis, pneumonia, rheumatism, gastrointestinal diseases, and other diseases are treated with badan leaves in traditional medicine. Mongolian medicine uses badan as a treatment for nausea and vomiting. During several growing seasons, one plant has green, red, and black leaves. The black leaves used in our study contain substances that exhibit adaptogenic, antistress, antioxidant, and immunomodulatory effects [17].

The aim of the study was to obtain PHMGH hydrogel compositions with *B.crassifolia* extract and study their

effects on thermal burn wound healing in rats.

EXPERIMENTAL

Monomers: Guanidine hydrochloride (GHC) produced by «Across Organics» was used without pre-purification (99%, T_m= 185-189 °C, [H_2O] ≤0.2%). Hexamethylenediamine (HMDA) was purified by distillation at 205 °C; the fraction was collected at 202-205 °C. 10% Formalin solution (Serosep HistoPot) was used. HMDA was purified by distillation at 205 °C; the fraction was collected at 202-205 °C.

Hydrogel synthesis: PHMGH was obtained by adding 10 - % formaldehyde solution to the polymer solution (C=30 g/dL) in fivefold excess relative to the number of terminal amino groups [8]. A one-hour reaction was run at room temperature. We purified the hydrogel from the sol fraction by washing the filtrate with distilled water on a Buchner funnel, with the refractive index of the filtrate being controlled to equal the refractive index of water.

Determination of the equilibrium degree of swelling: The equilibrium swelling hydrogel (Q_p) was determined by the gravimetric method [18]. The swollen hydrogel samples were weighed and placed into a desiccator after drying.

The calculation was carried out according to the formula:

$$Q_p=(m_1-m_2)/m_2$$

where m_1 is the mass of the swollen gel, m_2 is the mass of the dry gel.

The study of pH sensitivity of hydrogel: We determined the dependency of Q_p on pH using an IZMTEH I-160MI laboratory ionometer. By adding the required amount of HCl, the pH of the medium was smoothly changed to the acid side.

Herbal raw materials: The black leaves of *B.crassifolia* (L.) Fritsch were used in the study. The black (overwintered) leaves of *B.crassifolia* were collected in October 2019 on the coast of Lake Baikal (Republic of Buryatia). The samples were delivered to the Biotechnological Center of East Siberian State University of Technology and Management (Ulan-Ude, Russia). The collected leaves were straightened, sorted, washed in cold water and laid out for air drying in a dry, warm and ventilated room for 48-60 hours. Turning the leaves over three or four times a day prevented mold growth and rot. The dry plant material was stored in a paper bag. To prepare the extract, the dry leaves were crushed to 3-5 mm.

Preparation of plant extracts: In research used pharmacy materials, such as leather bergenia leaves (*Bergenia crassifolia* (L.) Fritsch.) in the study. Plant extracts were prepared according to the pharmacopoeia article GPA.1.5.3.0006.15 of the State Pharmacopoeia in XIII edition named “Extractable Assay Test in Tedicinal Plant Materials and Herbal Medicines” (method 1). About 1g of powdered drug plant material (exact amount) was sifted through sieve with 1mm hole diameter and placed in a conical flask (capacity about 200-250 ml), after that it was added 50 ml of water, flask was plugged with a stopper, weighed (accurate to ±0.01 g) and left for 1 h. The flask then was joined with reflux and heated up on boiling water bath. The flask with content after cooling was plugged with the same stopper and weighted. Loss in weight of the flask content was cured by the same solvent. Flask content was thoroughly shaken and filtered through dry paper filter into a dry flask with capacity about 150-200 ml. 25 ml of the resulted filtrate was pipeted into a 50-70 ml porcelain casserole which was predried at a temperature of 100-105 °C to a constant weight. After that the content of a porcelain casserole was evaporated on water bath to dryness. Casserole with solid residue was dried to a constant weight at a temperature of 100-105 °C, also it was cooled for 30 minutes in desiccator with anhydrous calcium chloride at the bottom and immediately weighted.

Preparation of the hydrogel composition: Composites were prepared by immersion of a 1g sample weight into solutions of plant extracts for different intervals (15, 30, 45, 60, 75 min.). Sample weights were removed and dried at an ambient temperature to a constant weight after hydrogel was held in plant extracts.

Quantitative analysis was treated by using a Milichrom A-02 microcolumn liquid chromatograph (Ekonova, Novosibirsk, Russia) on a ProntoSIL-120-5-C18 AQ column (2 × 75 mm, 5 μm; Metrohm AG, Herisau, Switzerland); moving phase: 0.2 M $LiClO_4$ in 0.006 M $HClO_4$ (A), MeCN (B). Gradient (% B): 0 - 6 min 10 - 20%, 6 - 9.3 min 20%, 9.3 - 10 min 20 - 30%, 10 -14 min 30 - 35%, 14 - 16 min 35 - 55% (*B.crassifolia* leaves); 0 - 5 min 11 - 18%, 5 - 9 min 18%, 9 -10 min 18 - 20%, 10 - 12 min 20 - 25%, 12 - 16 min 25%, 16 - 20 min 25 - 100% (*Calendula’s officinalis* flowers); 0 - 27 min 5 - 10% (*Tussilago farfara* leaves). Separation was performed at a flow rate of 150 μl/min and at a column’s temperature of 35°C.

Detection was performed with UV-detector at a distance of 270 nm (*Bergenia crassifolia* leaves) and 330 nm (*Calendula officinalis* flowers and *Tussilago farfara* leaves). Ratio-method was provided with such reference materials as a: gallic acid (>96%), arbutin (>97%), bergenit (>95%), 3-O- caffeoylquinic acid (>93%), 4-O- caffeoylquinic acid (>95%), 3,4-di-O-caffeoylquinic acid (>92%), 4,5-di-O- caffeoylquinic acid (>94%), 3.5-di-O- caffeoylquinic acid (>90%), 1.3-di-O- caffeoylquinic acid (>95%; all Sigma-Aldrich). Narcissine (>95%) and typhaneoside (>92%) were extracted arlier. The results are depicted in mean of 5 parallel definitions (± standard deviation, SD). Sample preparation was provided by transferring accurate weight of gel (80 mg) into the Eppendorf tube (2 ml), adding 1 ml of water and treating by ultrasonic (50 kHz, 30 min, 40°C). After all sample was centrifuged (6000 g, 20 min). Obtained extract was filtered through membrane filter (0.45 μm) and used for assay (1 μl).

FTIR spectroscopy, TG analysis and DS calorimetry: Fourier-transform infrared spectroscopy (FTIR) (ALPHA (Bruker, Germany) with attenuated total reflection attachment (ZnSe crystal), 4000-600 cm^{-1}) and data of thermogravimetric analysis and differential scanning calorimetry (TG/DSC) (STA 449 F3 Jupiter (NETZSCH, Germany); 5 °C/min, N_2/O_2 atmosphere) were obtained using the equipment of the Collective Use Center of Buryat Scientific Center, Siberian branch, Russian Academy of Sciences.

Determination of toxicity: Acute toxicity studies were conducted on 50 white male mice weighing 18-24 g obtained from the East Siberian Institute of Medical and Ecological Research (Russia, Angarsk). After the animals underwent a two-week quarantine, they were kept under normal vivarium conditions (room temperature 20-22 °C, relative air humidity 60-65%). Groups of 10 mice were kept in metal cages. Wood sawdust served as bedding. The cages were cleaned 2 times a week. The mice were fed a mixed diet of porridge, grains, and vegetables. Tap water was used for drinking.

The experimental animals were divided into 5 groups:

I - control group;
II - animals treated once with 1000 mg/kg hydrogel;
III - animals treated once with 3000 mg/kg hydrogel;
IV - animals treated once with 5000 mg/kg hydrogel;
V - animals treated once with 8000 mg/kg hydrogel.

These experiments were carried out according to requirements for preclinical studies of new drugs' general toxic effects [19].

The day before the experiment began, the animals were deprived of food. Using individual controlled feeding, the test substance was administered as part of the feed as a mixture with a small amount of porridge.

The experiments started at the same time in the morning. The animals were evaluated based on the following criteria: appearance, coat condition, behavior activity, changes in coordination of movements, gait, water and food consumption, excretion, etc.

After the observation period (14 days), the experimental and control animals were decapitated under light ether anesthesia and weighed. The internal organs were examined macroscopically and weighed after the autopsy. Using Statistica 6.0 software, parametric analyses were conducted on research results.

Thermal burn simulation: Experimental burn modeling was performed in the vivarium of East Siberian State University of Technology and Management on 40 outbred white rats weighing 180 - 200 g of both sexes. The animals and the vivarium were kept in accordance with Rules of Laboratory Practice (GLP), Order of the Ministry of Health of Russia dated April 1, 2016 N 199n "On Approval of the Rules of Good Laboratory Practice" and SP 2.2.1.3218-14 "Sanitary requirements for the device, equipment, and maintenance of experimental biological clinics (vivariums)". Based on sex, age, weight, and randomization, the animals were divided into five groups:

I - intact group (water ad libitum);
II - control group (burn and self-healing);
III - group of animals (burn and treatment with PGMGH hydrogel and *B.crassifolia* extract, complex preparation);
IV - group of animals (burn and treatment with *B.crassifolia* extract);
V - group of animals (burn and treatment with a reference drug based on chloramphenicol and methyluracilused).

This experiment was conducted according to the Federal Law dated 27 Dec., 2018 "On the Responsible Treatment of Animals and on Amendments to Certain Legislative Acts of the Russian Federation" and "Rules adopted by the European Convention for the Protection of Vertebrate Animals" (Strasbourg, 1986). During ether anesthesia, the animals underwent a thermal burn with a hot water solution at about 100°C after hair removal in the right lateral area [19].

The burn depth covered the subcutaneous layer after ten seconds of exposure. Exposure caused a burn with a degree of II (III "a" in the Russian Federation), covering 4-5% of the body surface. The day of wound inflicted was considered as day zero (dpt - day post treatment). The burn wound area was 5.0-6.0 cm^2. After removing the burn scab on the burn surface, the animals were treated with the drugs the next day. The research protocol was approved by the Ethical Commission of the East Siberian State University of Technology and Management (Protocol No. 3 of 02.02.2019).

Wound dressings were not removed until the surface of the wound had healed completely. Vulnography was used to determine wound healing. The wound size, appearance, type of discharge, and time for complete healing of the wounds were all assessed each day using a transparent film and graph paper [20]. Various dosage forms were analyzed on dpt 6, 13 and 20 after injury to determine how they repaired the wound and affected its surface.

Histological analisys: On the 6, 13, and 20 dpt, rats were phased out (2, 3, 3 animals) from the experiment using chloroform vapors. They took blood from the femoral artery, and after euthanasia, skin tissue samples were taken, placed in a 10% formalin solution, which was neutral. After that, they were washed in running water for 24 hours, followed by wiring and pouring into paraffin blocks. 50 sections were analyzed for each animal. Histological sections with a thickness of 7 μm were stained with hematoxylin and eosin according to Ehrlich and picrofuchsin according to Weigert and examined according to the Van Gieson method.

Axiostar plus microscope and a video camera for MICROCAM microscope were used to measure the thickness of the skin and other cellular inclusions such as epidermis, dermis, epithelium of hair follicles, and leukocyte count in the blood, granulation tissue and the number of fibroblasts.

An analysis of correlation was conducted within experimental groups according to Pearson's test. A statistical analysis of the resulting digital data was conducted using MS Excel. Following the generally accepted method, an Axiostar plus trinocular microscope was used in eight fields of view for counting fibroblasts. Based on the Student's test [21], significant results were determined as $P < 0.05$.

Blood test: Blood was collected from the animals on the 7, 13, and 20 dpt of the experiment in a test tube containing heparin (50 units/ml). A summary antioxidant activity (SAA), total leukocyte and erythrocyte content, catalase enzyme activity, and malondialdehyde content were determined. Using the amperometric method, the SAA of blood serum of the animals was determined on a liquid chromatograph "Tsvet-Yauza-01-AA". The mass concentration of water-soluble antioxidants was measured based on the calibration plot of signal output versus quercetin concentration [22].

Goryaev chamber was used to count the leukocytes in blood diluted with 3% acetic acid stained with methylene blue [23]. When blood was diluted with saline, the total number of erythrocytes was determined in Goryaev chamber.

The total erythrocyte counts in whole blood were determined by counting in the Goryaev chamber when diluted the blood with saline solution [23].

The permanganate method (according to Bach and Zubkova) was used to measure catalase activity in the blood. Catalase number is an indicator of enzyme activity [24].

The concentration of malondialdehyde in blood serum was determined using the method of M.Uchiyama and M.Michara [25, 26].

According to the generally accepted method, Axiostar microscopes (Germany) were used in 12 fields of view to count fibroblasts. In addition, the rate of healing of burn injuries was measured by the daily decrease in the area of the wound, calculated by the formula:

$$S = \frac{(S_1 - S_n) \times 100}{S_1 \times t}$$

where S_1 - is the size of the wound at the first measurement (dpt 0); *Sn* - is the size of the wound at the subsequent measurement (*i.e.*, 3, 5 dpt and etc.); *t* - is the number of days between the first and subsequent measurements. A percentage of the animals with healed wounds was also recorded.

The results were statistically analyzed using the Biostat-2006 program. The results were represented by a median Me, upper and lower quartiles Q1–Q3. The significance of differences was determined using the Mann–Whitney test. We considered the results significant when a level of difference was reached $p \leq 0.05$.

RESULTS AND DISCUSSION

PHMGH-based hydrogels were obtained by cross-linking the amino groups of PHMGH with formaldehyde [27]. By using a cross-linking agent, it is possible to increase the yield of the product to 70-80%, compared to some hydrogels produced by long-term polycondensation of monomers close to stoichiometric ratios (yield 45%). Additionally, the conditions for its production are milder, requiring less time, which is more suitable for commercialization. For spatially cross-linked structures, a polymer with a large number of terminal amino groups is essential for further interaction with aldehydes at the first stage. This led to branched PHMGH being synthesized at a ratio of 1 monomer (GHC) to 1.4 monomer (HMDA) [8]. The polymer was further treated with formaldehyde to produce a hydrogel.

Based on the FTIR spectra of the polymer and the hydrogel obtained (Fig. 1), a band of stretching vibrations of amino groups is observed at 3250 cm^{-1}. However, the intensity of the band decreases for the hydrogel during interaction with formaldehyde. This could be explained by the consumption of terminal amino groups of the polymer.

Since a methylene bridge binds the terminal amino groups, nitrogen atoms exhibit a negative inductive effect, increasing the polarity of the $-CH_2$ group, blocking scissor deformation vibrations (1460 cm^{-1}), while inducing wagging and torsional vibrations between 1300 cm^{-1} and 1270 cm^{-1} (Fig. 2).

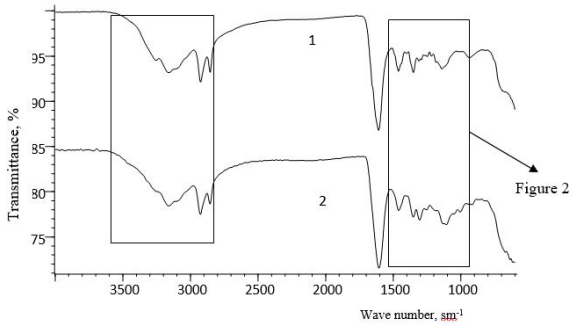

Fig. 1. IR spectra. 1-PGMGHC, 2-hydrogel

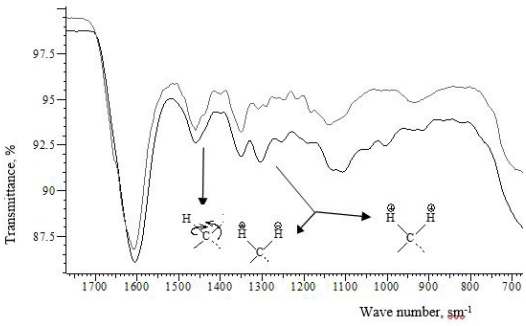

Fig. 2. Enlarged image of IR spectra. 1-PGMGHC, 2-hydrogel

In this gel, both branching and crosslinking centers are substituted hexahydrotriazine rings formed by aldehyde acting on the terminal -NH_2 of the water-soluble precursor (PHMGH) as well as branching centers already present in the precursor at the third amino group of HGC. Each of the substituents is a linear fragment of PHMGH.

In addition, TG/DSC analysis of the hydrogel allowed evaluation of the polymer's thermooxidative degradation. In Fig. 3 weight loss is observed at 100°C due to evaporation of water from the hydrogel sample. Thermal degradation of the polymer begins at 180°C. There follows stepwise destruction, probably due to successive destruction of the hexahydrotriazine ring, the guanidine group, and the thermal-oxidative destruction of aliphatic residues.

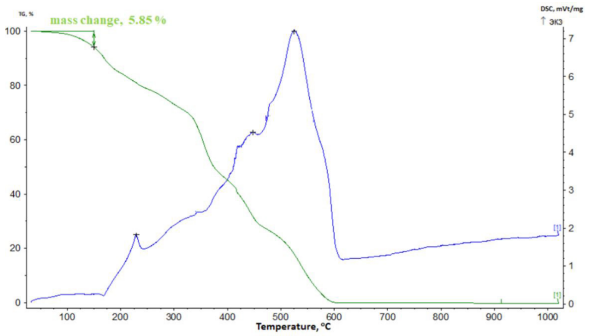

Fig. 3. TGA / DSC curves of the PGMGHC hydrogel

Based on the above, the hydrogel can be represented schematically as follows:

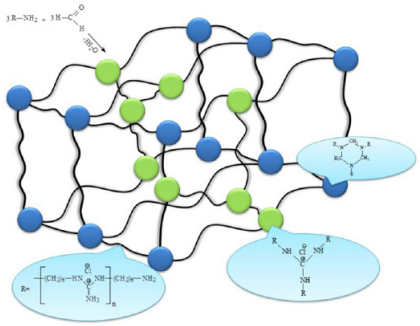

Scheme 1. Reaction of the preparation of the PGMGHC hydrogel

Swelling ratio of hydrogel: Swelling is one of the key characteristics of hydrogels. Hydrogels swell due to their porous structure, flexible polymer chain sections, high crosslink density, and affinity for solvents. Ionic hydrogels are prone to swelling because of osmotic pressure, which is generated by dissociation, as well as electrostatic repulsion between chain sections with the same charge. It is possible to control swelling by changing the solvent composition, for instance, by adjusting pH. Fig. 4 shows the sensitivity of the resulting hydrogel to pH.

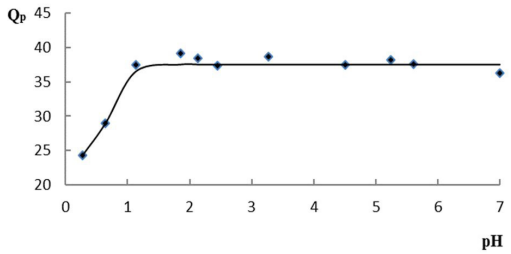

Fig. 4. Dependence of the equilibrium degree of swelling Q_p of the PGMGHC hydrogel on the change in the pH of the medium

The pH range from 1.2 to 7 did not affect Q_p. Hydrolysis of the hydrogel in an acidic environment leads to decomposition into fragments of the original polymer, which in turn is not a disadvantage since the released PHMGH fragments inhibit the growth of pathogenic bacteria. This leads to the fact that the released fragments of PHMGH inhibit the growth of pathogenic bacteria due to their antiseptic activity [28].

Hydrogel toxicity: All chemicals are classified according to their toxicity and other derived characteristics [29]. Such studies allow evaluation of their safety in practical use, which is one of the main requirements for wound healing drugs due to their direct contact with the patient.

According to results of toxicological studies performed in the study, the animals receiving the hydrogel by single feeding in the studied doses (1000, 3000, 5000, and 8000 mg/kg) did not die during the observation period (14 days).

During the entire observation period, the experimental animals did not differ from the control group in appearance, behavior, coat condition, intake of water and feed, and excretion. There were some deviations in body weight and growth from control indicators in animals treated with the drug, but these changes were not statistically significant (Table 1).

Table 1. Body weight and weight gain of white mice in the control and experimental groups with a single injection of PGMGH hydrogel in different doses (M ± m)

Indicators	Groups of animal				
	I	II	III	IV	V
Initial body weight, g	19.1±0.6	21.8±0.8	19.7±0.7	19.8±0.8	21.1±0.9
Body weight after 14 days, g	23.4±0.7	26.2±0.5	23.9±0.6	23.8±0.7	25.5±0.5
Body weight gain after 14 days,%	22.5±1.4	20.2±1.1	21.3±1.9	20.2±1.5	20.9±2.1

Neither the experimental nor control groups showed any differences in the macroscopic appearance of their internal organs. The internal organs of the animals showed no pathological changes.

The relative mass ratios of the internal organs in the control and experimental groups are shown in Table 2. Although the internal organ masses of the control

and experimental groups differed slightly, no significant differences were observed.

Table 2. Coefficients of the mass of the internal organs of white mice in the control and experimental groups with a single injection of PGMGH hydrogel at different doses (M ± m)

Indicators	Groups of animal				
	I	II	III	IV	V
Heart	0.56±0.04	0.45±0.08	0.48±0.03	0.48±0.06	0.46±0.04
Liver	4.54±0.18	4.15±0.19	4.37±0.13	4.50±0.20	4.08±0.13
Spleen	0.27±0.03	0.33±0.05	0.30±0.04	0.28±0.02	0.32±0.08
Kidney	1.32±0.05	1.29±0.04	1.18±0.07	1.27±0.05	1.18±0.08

In an acute experiment on mice fed PHMGH/ formaldehyde hydrogel at doses of 1000, 3000, 5000 and 8000 mg/kg, lethal outcomes were not observed, so the semi-lethal dose (LD_{50}) was not determined. We conclude from the studies conducted that this substance is practically non-toxic and can be classified as hazard class V according to GOST 32419-2013 ($2000 < LD_{50} \leq 5000$).

The chemical composition of B.crassifolia extract: In the experiment the hydrogel composition with black leaf extracts of *B.crassifolia* (complex preparation) was obtained. Compositions were received by holding hydrogel in solutions of plant extracts for different intervals [30]. During the sorption of *B.crassifolia* extract compounds the largest values (82.45%) were reached for gallic acid held in solutions for 75 min, concentration of arbutin (23.86%) and bergenin (17.14%) was roughly the same for all the time (Table 1). As gallic acid is a component of tannin esters, which exhibit an antioxidant effect both in oral and external applications [14]. In the future this may have a beneficial effect on wound healing.

The experiment modeled on a thermal burn: In the experiment modeled on a thermal burn was applied to laboratory animals as a wound healing agent.

Data on the dynamics of changes in the area of the wound are presented in Fig. 5.

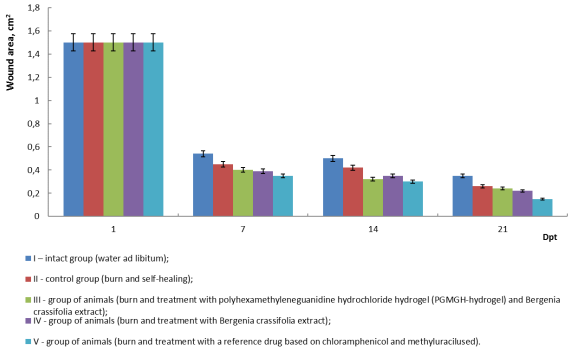

Fig. 5. Dynamics of wound healing in rats with thermal burns. Experienced groups: 1-control; 2-ointment based on chloramphenicol and methyluracil; 3-PGMGHC hydrogel; 4-*B. crassifolia* extract; 5-composition

The animals of group V had the minimum wound surface area at the end of the experiment. In this study, the complex preparation was used, which has a wound healing effect due to the antibacterial action of the guanidine-containing hydrogel and the antioxidant activity of the extract. Starting on the 3 dpt of the experiment (visual control), the area of wounds on the animals of the experimental groups was statistically significantly different from those of the control group. The animals of the experimental group **I** showed the greatest decrease in wound area. We have obtained preliminary data on morphological analysis of burn wound healing in rats. According to histomorphological analysis, all experimental animals exposed to thermal exposure developed the same type of thermal burn **III** "a" degree. The same destructive and dystrophic processes were observed in all layers of the skin, with the loss of all hair follicles, sweat glands, and sebaceous glands. All skin layers and subcutaneous muscle fibers underwent coagulation necrosis in most areas of the wound surface. A morphofunctional study of epidermis, dermis, and subcutaneous tissue was carried out in intact animals. Skin consists of two layers, the dermis and the epidermis, which are separated by the basement membrane and pass through the subcutaneous fatty tissue without sharp borders (Fig. 6).

The histological sections clearly show hair follicles and sebaceous glands with excretory ducts (Fig. 7).

The bulk of cellular elements are fibroblasts and fibrocytes. There are areas where polyblasts are forming. In the connective tissues of the skin, microscopy revealed blood vessels (small capillaries and large veins) as well as fibrocytes and fibroblasts. Hair follicles with growing epithelium were observed in large numbers in the dermis.

On the 6 dpt of the experiment, the histology of the burns was most prominent in the control group (with "natural healing" of wounds). In microscopy, epidermal tissue displays coagulative necrosis. Epidermis covers the inflammatory area. Infiltration with total necrosis follows thermal damage. Hair follicles and sebaceous glands are observed locally. In the epidermis, there is purulent exudate (Fig. 9). Leukocyte layer thickness reaches 404.07 μm, and its average value is 253.75 **μ**m.

Dead leukocyte cells, stratum corneum peeling, and young polyblasts form this layer. In addition, fibrocytes and fibroblasts were observed in small numbers. As well, there are deep destructive and dystrophic processes in all layers of the epidermis, resulting in blurring of the boundaries between them.

According to the study, the thickness of the granulation tissue on the 13 dpt of the experiment was not determined in the control group. An inflammatory scab with granulation areas was observed throughout the wound injury in the control group on the 20 dpt, and its dimensions averaged 1085.40 ± 33.50 **μ**m ($p<0.05$). Polymorphic leukocyte shafts were also observed,

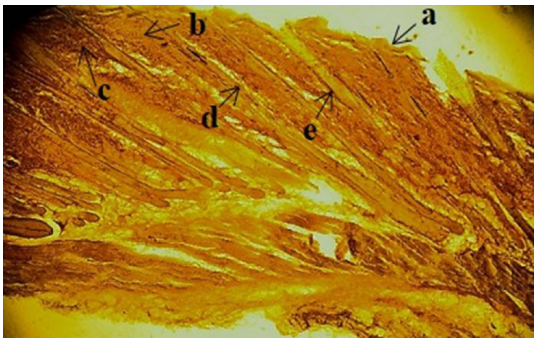

Fig.6. Intact group of animals, stratified squamous epithelium of the epidermis, hair shafts, a-horny, b-granular, c-prickly, d-papillary layers, e-epithelium of hair follicles (10x10)

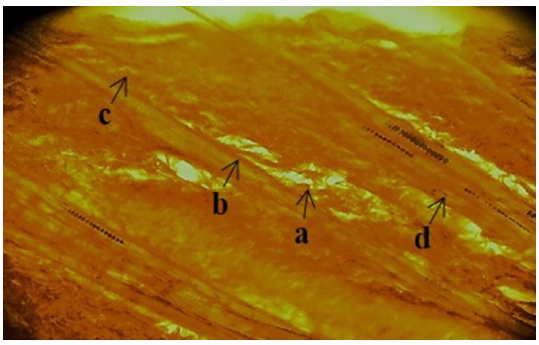

Fig. 7. Hair follicles with sebaceous glands and fibroblast cells and fibrocytes (intact group). a-sebaceous glands, b-follicle epithelium, c-horizontal vascular loops, d-fibroblast cells of the dermis (20x10)

limiting the scab from the wound surface at a height of 166.00 ± 0.62 μm. Rats' immune systems responded by infiltrating wounds and activating macrophages.

As compared with the other two experimental groups, the healing process of the burn wound was most effective in the group **III** on the 6 dpt of the experiment, when 100 mg of a complex preparation was applied daily to the wound area. Based on the microscopic examination, wound defects have been reduced more rapidly.

There was a less pronounced inflammatory response to wounds in the epidermis of animals in this group. In the control group (with "natural healing" wounds), the scab was thinner. During epithelialization, epithelium grew on the wound surface from the epithelial cells at the wound's edges and in the deep layers of the skin with granulation tissue forming by secondary intention (Fig.11).

However, this group of animals shows less pronounced edema of the dermis and hypodermis than the control group. Under the scab, a layer of stratified epithelium is visible beneath the inflammatory tissue. Compared to the control group, the experimental group **I** formed granulation tissue more rapidly and the burn area was partially covered by epithelium. During epithelization, epithelium grows from the edge of the wound toward the surface of the wound (Figs. 12, 13).

A different histological picture was observed in sections of thermal burns of the experimental group **IV** of animals treated with *B.crassifolia* extract than in sections from other experimental groups. There was local purulent exudate with penetration into the deep dermal layers on the 6 and 13 dpt in the area of thermal burn.

Upon treatment of burns with the extract of *B.crassifolia* thick-leaved, the affected area showed a clearly developed macrophage reaction. In a laboratory study of sections taken on the 20 dpt of the experiment, no signs of hyperemia or edema were observed in the group **IV** of animals. Connective tissue of the regenerate was mature, clean, and structurally similar to healthy skin of intact animals. A slight pink granulation tissue filled the outer surface of the skin and had an average thickness of 1287.41 ± 33.50 μm ($p<0.05$). Dermis revealed numerous areas with hair follicles with thin epithelium with an average thickness of 7.73:0.86 μm ($p=0.05$) (Figs. 15, 16).

In the experimental group **V** of animals treated with chloramphenicol and methyluracil ointment, thin layers of scab with signs of necrosis were observed on the 6 dpt (Fig. 17).

There was a purulent exudate with local skin peeling on the surface of the epidermis on the 13 and 20 dpt. It was noted on the 20 dpt of the experiment that the burned area was covered with an epithelial layer, and a slight hyperemia persisted without signs of edema. Epithelium edges are uneven and pathological processes continued in the experimental group treated with ointment containing chloramphenicol and methyluracil. The epithelium of hair follicles was thin at 11.01+1.27 μm, while the leukocyte-necrotic scab in the area of inflammation had an average thickness of 106.25 ± 11.58 μm (Figs. 18, 19).

As a result, the complex preparation had a greater reparative effect than the reference drug and the aqueous extract of *B.crassifolia.*

Blood test: The pathogenesis of burn disease is strongly influenced by decreased antioxidant activity (AOA). In burns, AOA levels decrease significantly in blood serum and membranes of erythrocytes, providing indirect confirmation of a decrease in endogenous antioxidant levels [31, 32].

Based on Table 5, burns (control group (**II**)) showed a decrease in SAA**.** Compared with the norm (intact animals), dynamics were 18, 24, and 5% on the 6, 13, and 20 dpt. The complex preparation, badan extract and ointment based on chloramphenicol and methyluracil used during treatment resulted in an increase in SAA, and the process of restoring this indicator was most pronounced in the experimental group **III**. The damage caused by burns increases the number of leukocytes (leukocytosis). Moreover, the literature describes two waves of leukocytosis. During the first 6 - 12 hs after injury, the total number of leukocytes reaches a maximum and lasts for three days before decreasing. On the 5 and 10 dpt, the second wave begins and lasts 3-8 days, while the maximum number of leukocytes is usually lower in this wave [33].

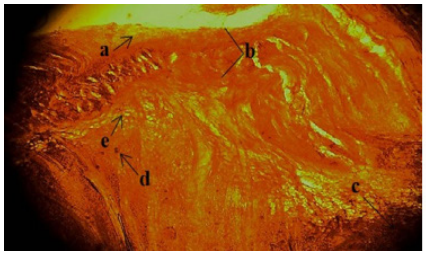

Fig. 8. Histological picture of the burn in the control group (6 dpt). There is coagulation necrosis of the epidermis, blurring of the boundaries between the layers, a-purulent exudate, b-leukocyte-necrotic layer, c-coagulation necrosis of connective tissue with symptoms of edema and infiltration, d-residues of the sebaceous glands, e-horizontal vascular loops (10x10)

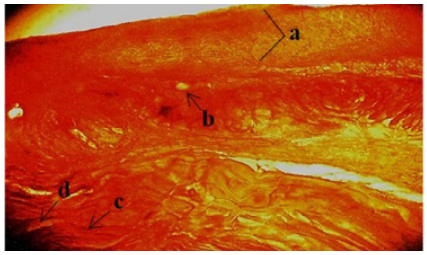

Fig. 9. Group II, severe hyperemia, edema wit infiltration and plethora of blood vessels, a-leukocyte-necrotic scab, b-small purulent exudate, polyblast cells, d-hair follicles (20 dpt) (10x10)

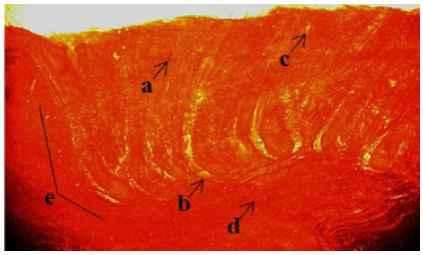

Fig. 10. Group II on dpt 20, local formation of hair follicles and pronounced purulent exudate. Horizontal and vertical vascular loops: a-single fibroblasts, b-hair follicles, c-sebaceous gland residues, d-polyblasts, e-granulation tissue (10x10)

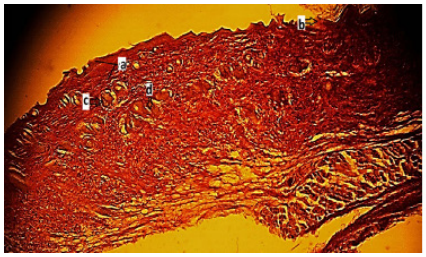

Fig. 11. Group III with less pronounced hyperemia and a thin layer of purulent exudate (6 dpt), a-leukocyte-necrotic layer, b-purulent exudate, c-remnants of hair follicles, d-vascular loops (10x10)

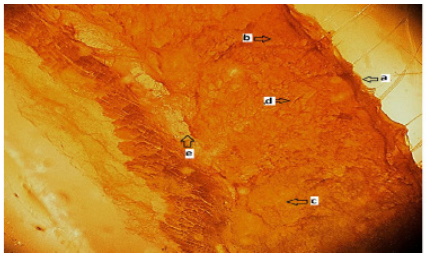

Fig. 12. Treatment of a burn wound with a group III, mature epidermis with hair follicles and growing epithelium: a-horny, b-granular, c-prickly, d-papillary, e -basal (10x10)

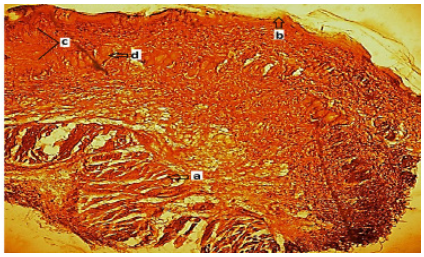

Fig. 13. A large number of hair follicles in the dermis and a small amount of decreasing purulent exudate at the bottom of the burn: a-mesh layer, b-local purulent exudate, c-granulation tissue, d-hair follicles (10x10)

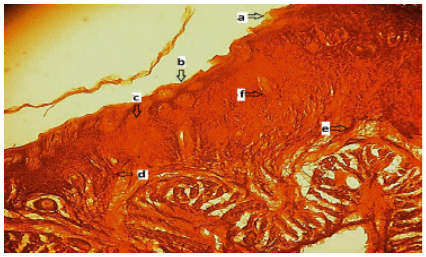

Fig. 14. Group IV: a-purulent exudate, b-horny, c-granular, d-prickly, e-basal, f-papillary layers (10x10)

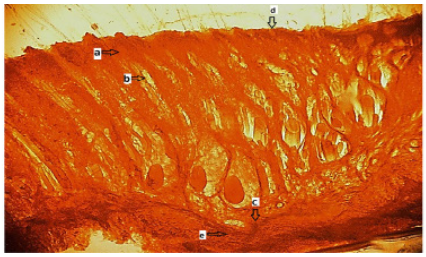

Fig. 15. Treatment with group IV. Mature epidermis with hair follicles: a-granular, b-papillary, c-prickly, d-horny, e-basal layers (10x10)

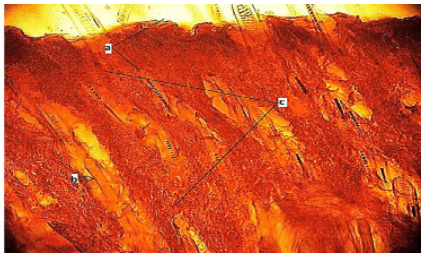

Fig. 16. Treatment of a thermal burn with group IV: a-leukocyte-necrotic layer, b-hair follicles, c-granulation tissue (10x10)

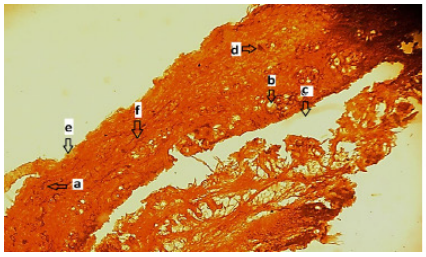

Fig. 17. Treatment of a burn wound group V. Detachment of the epidermis from its own skin (dermis), a-cells of fibroblasts, b-remnants of the sebaceous glands, c-exfoliation of the epidermis from the dermis, d-remnants of hair follicles, e-purulent exudate, f-blood vessel (10x10)

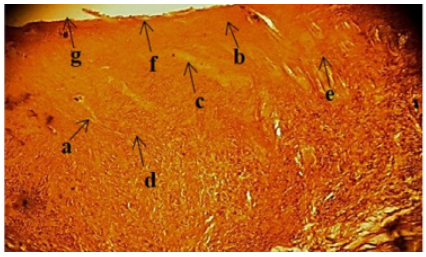

Fig. 18. Group V, visible five layers of the epidermis: a-prickly, b-granular, c-papillary, d-basal, e - fibroblast cells, f – horny, g - purulent exudate (10x10)

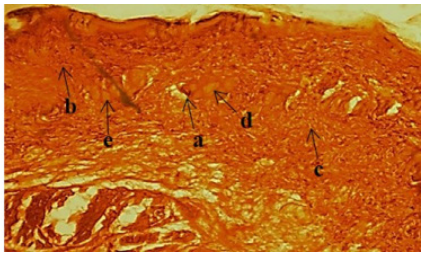

Fig. 14. Group V, dermis condition: a-sebaceous gland residues, b-blood vessels, c-vascular loops, d-hair follicle residues, e-hair follicles (10x10)

Table 4. Morphometric data of rat wounds after a burn on the 20 dpt of healing

Group	Epidermis thickness (mcm)	Derma thickness (mcm)	Epidermal / dermis thickness (mcm)	Granulation tissue thickness (mcm)	Fibroblasts of the dermis	Leukocyte-necrotic layer	Hair follicle epithelium
I	485.59±24.92	2039.49±104.65	2544.25±64.78	-	37.67±1.09	-	11.70±0.34
II	241.89±24.78^{*1}	1082.56±24.78^{*1}	1383.77±135.16^{*1}	2039,41±33.50	13.67±0.67^{*1}	166.00±0.67	7.73±0.86^{*1}
III	354.3±12.^{0*1,2}	1488.30±50.46$^{*1.2}$	1807.14±94.12^{*1,2}	2178.00±48.58	30.00±0.52^{*2}	85.39±9.83^{*2}	14.15±1.13^{*2}
IV	361.82±5.89^{*1,2}	1519.63±24.73^{*1,2}	1881.45±15.31^{*1,2}	1969.15±32.84	14.67±0.67^{*1,3}	187.35±7.02^{*2,3}	7.60±1.02^{*3}
V	358.15±15.49^{*1,2}	1504.23±65.06^{*1,2}	1851.60±40.27$^{*1.2}$	2268.00±30.43	27.17±0.87^{*1,2,4}	166.25±11.85^{*3}	11.01±1.27^{*2,4}

Table 5. SAA in blood serum from rats with thermal burns (Me (Q1-Q3))

Group	Dpt / SAA, mg/100 ml		
	6	13	20
II	31.35^{*n} (31.1-31.57)	29.17^{*n} (27.81-30.53)	36.11 ^{*n} (35.64-36.58)
III	34.20^{*n,2} (33.98-34.4)	36.05^{*2} (33.14-38.96)	40.03^{*2} (38.88-41.18)
IV	34.01^{*n,2} (33.39-34.63)	34.80^{*2} (32.05-37.55)	35.41^{*n,3} (35.05-35.77)
V	35.44^{*n,2,3}	34.09 ^{*n,2} (33.28-34.9)	34.40^{*n,2,3,4} (34.02-34.72)

According to our data (Table 6), the number of leukocytes increased in the control group (**II**) on the 6, 13, and 20 dpt by 24, 64, and 22%, respectively. As a result of the use of the studied drugs in the treatment, the number of leukocytes in the peripheral blood of rats was restored. The recovery process of this indicator was most pronounced in group **III** (under the action of a complex preparation) on the 13 and 20 dpt.

One of the oldest enzymes in the human body's antioxidant system, catalase belongs to a class of enzymes called oxidoreductases that catalyze redox reactions. Tables 7 and 8 present experimental data on catalase activity (catalase number and catalase index) in the blood of rats.

Table 6. Leukocyte count in the blood of rats during thermal burns (Me (Q1-Q3)).

Group	Dpt / Count of leukocytes x10^9/l		
	6	13	20
II	6.88 (6.17-7.59)	9.13^{*n} (8.82-9.75)	6.81^{*n} (6.37-7.25)
III	6.00 (5.54-6.47)	6.44^{*2} (6.06-6.84)	6.06 (5.68-6.44)
IV	6.75 (6.09-7.44)	6.87^{*n,2} (6.54-7.25)	6.54 (6.10-6.98)
V	5.58 (5.33-5.83)	6.84^{*n,2} (6.67-7.01)	6.38 (6.07-6.69)

Table 7. Catalase activity (catalase number) in rats with thermal burns (Me(Q1-Q3)).

Group	Dpt / catalase number, unit		
	6	13	20
II	10.73^{*n} (9.80-11.66)	9.41*^{n} (8.51-10.31)	10.47^{*n} (9.34-11.16)
III	12.33 ^{*2} (11.73-12.93)	11.33^{*n,2} (10.46-12.2)	12.98^{*2} (12.24-13.72)
IV	12.50^{*2} (11.91-13.09)	10.03^{*n} (9.24-10.82)	11.80^{*n,2,3} (11.37-12.23)
V	12.03 (10.81-13.25)	11.04^{*n,2} (10.42-11.66)	11.81 (10.96-12.66)

As follows from the data in Table 7, the burn (group **II**) led to a decrease in the catalase number on all days of the study (dpt 6, 13, and 20), which was below the norm by 16, 26, and 18%, respectively. As a result of treatment with all studied drugs, the catalase number in the blood of rats returned to normal. The recovery process of this indicator was most pronounced in group **III** (under the action of a complex preparation) on the 13 and 20 dpt. A catalase index can also be used to measure catalase activity, which is the ratio of catalase

Table 8. The catalase index in the blood of rats with thermal burn (Me).

Group	Dpt / Count of erythrocytes, mil. / 1 mcl blood / catalase index, *10^{-6}		
	6	13	20
II	6.70 / 1.60	5.85 / 1.61	6.01 / 1.74
III	6.50 / 1.90	5.62 / 2.02	5.99 / 2.17
IV	6.40 / 1.95	5.13 / 1.96	5.64 / 2.09
V	6.60 / 1.82	5.61/ 1.96	6.00 / 1.97

Table 9. The content of malondialdehyde (CMDA) in the blood serum of rats with thermal burns (Me (Q1-Q3))

Group	Dpt / C_{MDA}, mcmol/l		
	6	13	20
II	1.67*n (1.57-1.77)	1.78*n (1.64-1.92)	1.24 (1.17-1.31)
III	1.26*2 (1.16-1.35)	1.47*n,2 (1.44-1.50)	0.97*2 (0.81-1.13)
IV	1.36*2 (1.21-1.51)	1.52*n,2 (1.42-1.62)	1,21 (1.02-1.4)
V	1.31*2 (1.11-1.51)	1.48*n,2 (1.45-1.51)	1.01*2 (0.91-1.11)

activity to millions of erythrocytes in 1.0 μl of blood (Table 8).

As follows from the data in Table. 8, the complex preparation had the greatest reparative effect (group **III**). It significantly restored the catalase index on the 13 and 20 dpt ($p \leq 0.05$).

As a result of burn injury, lipid peroxidation (LPO) of biological objects changes. In order to assess the intensity of lipid peroxidation (LPO), malondialdehyde (concentration), which reacts with thiobarbituric acid to form a complex of active products, is widely used [34]. Their accumulation in tissues is one of the indicators of redox state disturbance and is a method for the early detection of metabolic disorders [35].

Table 9 shows the changes in malonic aldehyde levels in the experiment.

It follows from Table 9 that thermal burn (group **II**) caused an increase in the content of malonaldehyde in the blood serum of rats on the subsequent 6, 13 and 20 dpt, respectively, by 44, 53 and 7% compared with intact animals. During all dpt in group **III**, the most pronounced process of restoring this indicator was observed due to the use of a complex preparation.

CONCLUSIONS

Complex preparation were found to be effective in treating experimental animals with thermal skin burns, as they facilitated wound cleansing and accelerated healing. Additionally, they contributed to more intense healing of damage and the formation of granulation tissue than the pharmacopoeial preparation based on chloramphenicol and methyluracil, which was manifested in the inhibition of inflammatory processes with purulent-necrotic complications and the prevention of fiber degradation. According to the study, the hydrogel composition normalizes the total antioxidant and leukocyte activity and indicates a normal wound healing process. Due to the presence of natural antioxidants in the extract of *B.crassifolia*, the composition provides wound healing properties of its own, enhanced by the hydrogel's wound healing properties.

Accordingly, it has been shown that the use of a hydrogel composition containing the extract of *B.crassifolia* has a positive effect on the healing process of burns and opens up the possibility of developing new compositions using extracts of Baikal medicinal plants.

FUNDING

The study was performed within the framework of the state assignment of Baikal Institute of Nature Management Siberian Branch Russian Academy of Sciences No 0273-2021-0007.

AVAILABILITY OF DATA AND MATERIALS

The data analyzed during the study will be available from the corresponding authors upon request.

COMPETING INTERESTS

The authors declare that they have no competing interests.

REFERENCES

1. Abayev Yu.K. (2006) Surgeon's reference book. Wounds and wound infection. Feniks, Rostov na Donu. (In Russian)
2. Kajjari P.B., Manjeshwar L.S., Aminabhavi T.M. (2011) Novel interpenetrating polymer network hydrogel microspheres of chitosan and poly(acrylamide)-grafted-guar gum for controlled release of ciprofloxacin. *Ind. Eng. Chem. Res*., **50**(23), 13280-13287. https://doi.org/10.1021/ie2012856
3. Soppirnath K.S., Aminabhavi T.M. (2002) Water transport and drug release study from cross-linked polyacrylamide grafted guar gum hydrogel microspheres for the controlled release application. *Eur. J. Pharm. Biopharm*., **53**(1), 87-98. https://doi.org/10.1016/S0939-6411(01)00205-3
4. Liu H., Wang C., Li C., Qin Y, Wang Z., *et al*. (2018). Functional chitosan-based hydrogel as a wound dressing and drug delivery system in the treatment of wound healing. *RSC Adv*., **8**(14), 7533-7549. https://doi.org/10.1039/c7ra13510f
5. Anumolu S.S., Singh Y., Gao D., Stein S., Sinko P.J (2009) Design and evaluation of novel fast forming pilocarpine-loaded ocular hydrogels for sustained pharmacological response. *J. Controlled Release*, **137**(2), 152-159. https://doi.org/10.1016/j.jconrel.2009.03.016
6. Wu D.Q., Zhu J., Han H., Zhang J.Z., Wu F.F., *et al*. (2018) Synthesis and characterization of arginine-NIPAAm hybrid hydrogel as wound dressing: *In vitro* and *in vivo* study. *Acta Biomaterialia*, **65**, 305-316. https://doi.org/10.1016/j.actbio.2017.08.0488
7. Zinoviev E.V., Ivakhnyuk G.K., Dadayan K.A.,

Lagvilava T.O. (2014) Wound-healing effect of carbopol hydrogels in rats with alloxan diabetes model. *Experiment. Clin. Pharm.*, **77**(1), 20-25. (In Russian)
8. Ochirov O.S., Stel'makh S.A., Mognonov D.M. (2016) Hydrogels based on polyalkylguanidines and aldehydes. *Polym. Sci. Ser. B*, **58**(3), 334-340. https://doi.org/10.1134/S1560090416030106.
9. Grigorieva M.N., Stelmakh S.A., Astakhova S.A., Tsenter I.M., Bazaron L.U. *et al.* (2015) Synthesis of polyalkylguanidine hydrochloride copolymers and their antibacterial activity against conditionally pathogenic microorganisms *Bacillus cereus* and *Escherichia coli*. *Pharm. Chem. J.*, **49**(2), 29-33. https://doi.org/10.1007/s11094-015-1230-z
10. Stelmakh S.A., Grigor'eva M.N., Garkusheva N.M., Lebedeva S.N., Ochirov O.S., *et al*. (2021) Studies of new biocidal polyguanidines: Antibacterial action and toxicity. *Polym. Bull*., **78**(4), 1997-2008. https://doi.org/10.1007/s00289-020-03197-1
11. Vointseva I.I., Gembitskiy P.A. (2009) Polyguanidines - disinfecting agents and multifunctional additives to composite materials. LKM-Press, Moskow. 300 (In Russian)
12. Lebedeva S.N., Ochirov O.S., Stelmakh S.A., Grigor'eva M.N., Zhamsaranova S.D., *et al.* (2018) Reparative action of hydrogel polygexamethylenuanidine hydrochloride. *Bull. Sib. Med.*, **17**(1), 112-120. (In Russian) https://doi.org/10.20538/1682-0363-2018-1-112-120
13. Ochirov O.S., Olennikov D.N., Grigoreva M.N., Stelmakh S.A., Mognonov D.M., *et al*. (2019) Sorption capacity of a hydrogel based on polyhexamethyleneguanidine hydrochloride. *Farmacia*, **67**(3), 418-422. https://doi.org/10.31925/farmacia.2019.3.6
14. Tumova L., Endrychová H., Vokurková D. (2018) Immunostimulant activity of *Bergenia* extracts. *Pharmacognosy Magazine*, **14**(56), 328-332. https://doi.org/10.4103/pm.pm_423_17
15. Kim J., Lee C.M. (2018) Transdermal hydrogel composed of polyacrylic acid containing propolis for wound healing in a rat model. *Macromol. Res.*, **26**(13), 1219-1224. https://doi.org/10.1007/s13233-019-7014-7
16. Ochirov O.S., Razuvaeva Y.G., Badmaev N.S., Stelmakh S.A., Mognonov D.M. (2016) Wound-healing effect of polyguanidine-based hydrogel. *Acta Biomedica Scientifica,* **1(5)**, 117-120. https://doi.org/10.12737/23405 (In Russian)
17. Jarić S., Kostić O., Mataruga Z., Pavlović D., Pavlović M., *et al.* (2018) Traditional wound-healing plants used in the Balkan region (Southeast Europe). *J. Ethnopharm.*, **211**, 311-328. https://doi.org/10.1016/j.jep.2017.09.018
18. Mironov A.N., Bunatyan N.D. Vasil'ev A.N. *et al.* (2012) The guidelines for preclinical studies of drugs. Grif&K, Moskow. 944 (In Russian)
19. Paramonov B.A., Chebotarev V.Yu. (2002) Methods for modeling thermal skin burns in the development of drugs for topical treatment. *Bulletin of Experimental Biology and Medicine*, **134**(11), 593-597. (In Russian)
20. Ponomar' N.S., Maklyakov Yu.S., Khloponin D.P., *et al.* (2012). Effect of the ionized silver preparation on regeneration of the skin and underlying tissues in modelling thermal and chemical burns in rats. *Biomedicine*, **1**, 143-148. (In Russian)
21. Lakin G.F. (1990) *Biometry,* Vysshaya shkola, Moskow. (In Russian)
22. Yashin A.Ya., Mikhaylova T.A., Titov V.N., Suskova V.S., *et al*. (2015) Method and device for rapid determination of the patient's antioxidant status. *Instruments*, **6**, 32-39. (In Russian)
23. The methods of clinical laboratory testing. (2020), In: Kamyshnikova V.C. 10nd ed., MED-press-inform, Moskow. (In Russian)
24. Korolyuk M.A., Ivanova L.I., Mayorova I.G., *Tokarev V.E.* (1988) Method for determining the activity of catalase. *Clinical laboratory diagnostics,* **1**, 16-19. (In Russian)
25. Michara M., Uchiyama M. (1980) Thiobarbituric acid value on fresh homogenate of rat as a parameter of lipid peroxidation in aginy, CCL_4 intoxication and vitamin E deficiency. *Biochem. Med*., **23**, 302-311. https://doi.org/10.1016/0006-2944(80)90040-x
26. Uchiyama M., Michara M. (1978) Determination of malonaldehyde precursor in tissues by thiobarbituric acid test. *Anal. Biochem.*, **86**(1), 271-278. https://doi.org/10.1016/0003-2697(78)90342-1
27. Ochirov O.S., Mognonov D.M., Stelmakh S.A. (2015) Polymeric hydrogels based on polyhexamethylene guanidine hydrochloride and formaldehyde. *Rus. J. of Appl. Chem*., **88**(2), 332-335. https://doi.org/10.1134/S1070427215020238
28. Grigor'eva M.N., Stel'makh S.A., Astakhova S.A., Tsenter I.M., Bazaron L.U., *et al*. (2014) Biocidal action of copolymers based on aliphatic diamines and guanidine hydrochloride. *J. Appl. Polym. Sci*., **131**(11), 40319. https://doi.org/10.1002/app.40319
29. Saganuwan S.A. (2017) Toxicity studies of drugs and chemicals in animals: An overview. *Bulg. J. Vet. Med*., **20**(4), 291-318. https://doi.org/10.15547/bjvm.983
30. Ochirov O.S., Olennikov D.N., TurtuevaT.A., Grigor'eva M.N., Stel'makh S.A., *et al*. (2020) Sorption activity of hydrogels of polyhexamethylene guanidine hydrochloride regarding extracts of medicinal plants. *J. Phys.: Conf. Ser.,* **1611**(1), 012049. https://doi.org/10.1088/1742-6596/1611/1/012049
31. Mikhalchik E.V, Titkova S.M, Anurov M.V, Penkov L.Y, Korkina L.G. (2006). Antioxidant skin enzymes at experimental burns *Biomedical Chemistry*,

52(6), 576-586. (In Russian)
32. Mikhal'chik E.V., Lipatova V.A., Ibragimova G.A., Pen'kov L.Yu., Ibragimova G.A., *et al*. (2009) Activity of antioxidant enzymes in the wound in patients with deep burns. *Bull. Exp. Biol. Med.*, **147**(6), 753-756. https://doi.org/10.1007/s10517-009-0614-z
33. Paramonov B.A., Porembskiy Ya.O., Yablonskiy V.G. (2000) Burns: A guide for physicians. St. Petersburg, SpetsLit, SPb. (In Russian)
34. Arutyunyan A.V., Dubinina Ye.Ye., Zybina N.N. (2000) Metods for assessing free-radical oxidation and the antioxidant system. of the body. Methodical Recommendations. St. Petersburg, *IKF «Foliant»,* 93-94. (In Russian)
35. De Iuliis G.N., Newey R.J., King B.V. *Aitken R.J*. (2009) Mobile phone radiation induces reactive oxygen species production and DNA damage in human spermatozoa in vitro. *PloS ONE*, **4**(7), e6446.14. https://doi.org/10.1371/journal.pone.0006446